Mesenchymal stem cells ameliorate experimental autoimmune encephalomyelitis inducing T-cell anergy

Emanuela Zappia, Simona Casazza, Enrico Pedemonte, Federica Benvenuto, Ivan Bonanni, Ezio Gerdoni, Debora Giunti, Antonella Ceravolo, Francesco Cazzanti, Francesco Frassoni, Gianluigi Mancardi, and Antonio Uccelli

We studied the immunoregulatory features of murine mesenchymal stem cells (MSCs) in vitro and in vivo. MSCs inhibited T-cell receptor (TCR)–dependent and –independent proliferation but did not induce apoptosis on T cells. Such inhibition was paired with a decreased interferon (IFN)–gamma and tumor necrosis factor (TNF)–alpha production and was partially reversed by interleukin-2 (IL-2). Thus, we used MSCs to treat myelin oligodendrocyte glycoprotein (MOG)35-55–induced experimental autoimmune encephalomyelitis (EAE) in C57BL/6J mice. We injected intravenously 1 × 10^6 MSCs before disease onset (preventive protocol) and at different time points after disease occurrence (therapeutic protocol). MSC administration before disease onset strikingly ameliorated EAE. The therapeutic scheme was effective when MSCs were administered at disease onset and at the peak of disease but not after disease stabilization. Central nervous system (CNS) pathology showed decreased inflammatory infiltrates and demyelination in mice that received transplants of MSCs. T-cell response to MOG and mitogens from MSC-treated mice was inhibited and restored by IL-2 administration. Upon MSC transfection with the enhanced green fluorescent protein (eGFP), $eGFP^+$ cells were detected in the lymphoid organs of treated mice. These data suggest that the immunoregulatory properties of MSCs effectively interfere with the autoimmune attack in the course of EAE inducing an in vivo state of T-cell unresponsiveness occurring within secondary lymphoid organs. (Blood. 2005; 106:1755-1761)

Introduction

Stem cells have been viewed as a potential source of cells for any tissue due to their supposed capacity to give rise to virtually any type of cell. Among stem cells, stromal stem cells can be obtained from the bone marrow and induced to undergo differentiation in a variety of adult tissues. These cells have been indicated as mesenchymal stem cells (MSCs), can proliferate extensively in vitro, and differentiate under appropriate conditions in bone, cartilage, and other mesenchymal tissues[1] but also into multiple other cells derived from the 3 germ layers including neuroectodermal cells.[2-7] Upon tissue injury, MSCs have been shown to migrate to the damaged brain.[8] These results suggest that MSCs could provide an ideal cell source for repair of injured organs including the central nervous system (CNS).

In addition to their differentiation capability, MSCs have been recently demonstrated to suppress several T-lymphocyte activities, thus exerting an immunoregulatory capacity both in vitro and in vivo.[9,10] Though the mechanisms mediating such effects are still only partially understood, it is likely that mechanisms involving both cell-to-cell contact and soluble factors are involved in supporting T-cell inhibition in a noncognate fashion.[11-14]

MSCs can be easily obtained from human bone marrow upon bone biopsy, cultured in vitro, and administered to hematologic patients, providing help for the engraftment of hematopoietic stem cells.[15] In addition, allogenic human MSCs have been recently proposed for the treatment of acute graft-versus-host disease (GVHD).[16-18]

Experimental autoimmune encephalomyelitis (EAE) is an autoimmune inflammatory disease of the CNS that is mediated by T cells and macrophages and represents the paradigmatic model for multiple sclerosis (MS). In EAE, therapeutic approaches targeting T cells have been successfully used, leading to immunosuppression or tolerance. In this article, we report of the efficacy of MSCs isolated from C57BL/6J mice as treatment of EAE induced by the encephalitogenic peptide MOG35-55. This effect was due to a striking immune suppression on effector T cells occurring at the level of secondary lymphoid organs and leading to interleukin-2 (IL-2)–reversible T-cell anergy.

Materials and methods

Isolation, proliferation, and transfection of MSCs

Bone marrow from 6- to 8-week-old C57BL/6J mice was flushed out of tibias and femurs. After 2 washings by centrifugation at 1500 rpm (352 *g*) for 5 minutes in phosphate-buffered saline (PBS; Sigma-Aldrich, St Louis, MO), cells were plated in 75-cm^2 tissue-culture flasks at the concentration

From the Neuroimmunology Unit, Department of Neurosciences, Ophthalmology and Genetics, and the Centre of Excellence for Biomedical Research, University of Genoa, Genoa, Italy; and the Department of Haematology, San Martino Hospital, Genoa, Italy.

Submitted April 15, 2005; accepted May 10, 2005. Prepublished online as *Blood* First Edition Paper, May 19, 2005; DOI 10.1182/blood-2005-04-1496.

Supported by grants of the Italian Foundation for Multiple Sclerosis (A.U.), Istituto Superiore di Sanità (A.U.) "National Program on Stem Cells," the Fondazione CARIGE (A.U., G.M., and F.F.), and the "Compagnia di San Paolo" (F.F.).

An Inside *Blood* analysis of this article appears in the front of this issue.

Reprints: Antonio Uccelli, Department of Neurosciences Ophthalmology and Genetics, University of Genoa, Via De Toni 5, 16132–Genoa, Italy; e-mail: auccelli@neurologia.unige.it.

The publication costs of this article were defrayed in part by page charge payment. Therefore, and solely to indicate this fact, this article is hereby marked "advertisement" in accordance with 18 U.S.C. section 1734.

of 0.3 to 0.4 × 10^6 cells/cm^2 using Murine Mesencult as medium (Stem Cell Technologies, Vancouver, BC). Cells were kept in a humidified 5% CO_2 incubator at 37°C, and the medium was refreshed every 3 to 4 days, for about 4 to 5 weeks; then, only adherent cells were collected following 10-minute incubation at 37°C with 0.05% trypsin solution containing 0.02% ethylenediaminetetraacetic acid (Sigma-Aldrich). After the first cut and for the subsequent 4 or 5 passages, the cells were plated in 25-cm^2 flasks at 1.2 to 2.0 × 10^4cells/cm^2. For the following passages, cells were routinely seeded at 4 to 10 × 10^3 cells/cm^2 reaching confluence after 4 to 5 days.

MSC transfection was achieved with a second-generation lentiviral vector pRRLsin.PPT-hCMV engineered with the enhanced green fluorescent protein (eGFP) gene, with minor modification from the protocol described by Follenzi et al.[19] Briefly, 100 multiplicity of infection (MOI) of the eGFP vector was added to MSCs and cultured for 4 days, at which time about 70% of eGFP-positive cells was detected by flow cytometry.

Cell preparation and proliferation assays

Mononuclear cells (MNCs) for proliferation assays were obtained from the spleen and the lymph nodes of either healthy mice or EAE-affected mice 9 days after immunization. Cell suspensions were prepared using 70-μm filters (cell strainer-Falcon; Becton Dickinson, Franklin Lakes, NJ) and separating MNCs by ficoll gradient (Lympholite; Cedarlane, Hornby, ON). Cells were washed twice in PBS (Sigma-Aldrich) and suspended in complete RPMI medium containing 2 mM glutamine (Sigma-Aldrich), 100 IU/mL penicillin, 100 μg/mL streptomycin (ICN Biomedicals, Aurora, OH), 10% fetal bovine serum (FBS; Invitrogen/Gibco, Carlsbad, CA), and 50 μM β-Mercaptoethanol (ICN Biomedicals). Aliquots of MNC suspensions (2 × 10^5 in 200 μL) were seeded into 96-well, flat-bottomed microtiter plates (Sarstedt, Newton, NC) at a final cell density of 1 × 10^6/mL, in the presence of serial concentrations (1-10 μM) of the MOG_{35-55} peptide (Espikem, Florence, Italy), 2.5 μg/mL concanavalin A (ConA; ICN Biomedicals), or 10 μg/mL anti-CD3 antibody (R&D Systems, Minneapolis, MN) with or without 1 μg/mL anti-CD28 antibody (Pharmingen/Becton Dickinson Immunocytometry Systems, Palo Alto, CA). For experiments addressing the induction of anergy by MSCs, 100 IU/mL IL-2 (Pharmingen/Becton Dickinson) was added to the wells. In murine mixed lymphocyte reaction (MLR), MNCs were obtained from the spleen of C57BL/6J and CD1 mice. Effector cells from either C57BL/6J or CD1 mice were incubated with irradiated (30 Gy) feeder cells obtained, respectively, from CD1 or C57BL/6J mice. For human MLR, we used peripheral blood mononuclear cells (PBMCs) isolated from 2 healthy donors. Feeder cells were irradiated at 30 Gy and used to stimulate allogeneic PBMCs. In experiments addressing T-cell inhibition, concentrations of MSCs added to each well varied from 0.06 to 2 × 10^5 depending on experimental conditions. Supernatants from MSCs were derived from 3-day cultures, at 0.25 × 10^5 cells/well in 96-well plates, 2 days in Murine Mesencult and the last 24 hours in RPMI 10% FBS. Supernatant (100 μL) has been used for inhibition of proliferation in 200 μL total volume reaction. In every experimental condition, T-cell proliferation was studied after 72 hours of incubation in RPMI medium by standard ^{3}H-thymidine incorporation assay.

Cell-surface expression analysis

The following monoclonal antibodies (MAbs) directed against mouse surface markers anti-CD45 cytochrome C (CyC), anti–stem cell antigen-1 (Sca-1) phycoerythrin (PE), unconjugated anti-CD9, anti-CD3 CyC, anti-CD4 peridinin chlorophyll-alpha protein (PerCP), anti-CD73 PE, anti–major histocompatibility complex (MHC) class I PE, anti–MHC class II PE, and anti-CD11c allophycocyanin (APC) were purchased from Pharmingen/Becton Dickinson. Anti-CD11b fluorescein isothiocyanate (FITC), anti-CD3 PE, anti-CD69 FITC, anti-CD25 PE, anti-CD40 FITC, anti-CD80 FITC, anti-CD86 PE, and anti-CD34PE were all purchased from Serotec (Oxford, United Kingdom). Immunoglobulin G2b (IgG2b) anti–very late antigen-4 (VLA-4) supernatant was a generous gift of G. Constantin (Verona, Italy). Rat anti–mouse IgG1/2a FITC and anti–rat IgG2 FITC (Becton Dickinson) were used as secondary reagents for an indirect staining of $CD9^+$ and anti–VLA-4–positive cells, respectively. The phenotype of MSCs was routinely verified by flow cytometry using the following combinations of antibodies: CD11b FITC/CD34 PE/CD45 CyC and CD9 FITC/Sca-1 PE/CD45 CyC.

Regulatory T cells (TREGs) were identified by gating on $CD69^-CD3^+$ cells using anti-CD4 and anti-CD25 MAbs. MHC classes I and II as well as costimulatory molecule expression (CD40, CD80, and CD86) on $CD11c^+$ dendritic cells (DCs) were also evaluated. Analysis of TREGs and DCs was performed on cells derived from the spleen and lymph nodes of control and MSC-treated mice before disease onset at day 9 after immunization.

For all of these assays, cells were incubated for 30 minutes in the dark at 4°C. Afterward, they were washed once with PBS with 1% FBS, resuspended in 1 mL PBS, and immediately analyzed. All the analyses were performed using a FACSCalibur flow cytometer (Becton Dickinson). CELL Quest software (Apple, Cupertino, CA) was used for data analysis. Twenty-thousand events were acquired for each sample.

Immunostaining for apoptosis

Murine MNCs were stimulated in vitro with 10 μg/mL anti-CD3 (R&D Systems) or the lectin ConA (2.5 μg/mL), both alone and in the presence of MSCs, and harvested after 3 days for flow cytometric analysis of annexin V–positive apoptotic cells (MedSystems Diagnostics, Vienna, Austria). Briefly, cells were washed once with the "binding buffer" and first incubated with anti-CD3 PE-conjugated MAb in the dark for 30 minutes at 4°C. They were washed once and then incubated with FITC-labeled annexin V for 15 minutes in the dark at room temperature (RT). Next, cells were washed once, resuspended in 0.5 mL binding buffer, counterstained with propidium iodide, and analyzed. Total annexin V–positive cells were analyzed within the $CD3^+$ population.

Cytokine production

Quantitative analysis of interferon (IFN)–gamma, tumor necrosis factor (TNF)–alpha, and IL-4 levels was performed by enzyme-linked immunosorbent assay (ELISA) using commercially available kits (R&D Systems) on fresh supernatants derived from 3-day culture of MNCs stimulated by ConA, alone or in the presence of MSCs. IFN-gamma and TNF-alpha levels were measured at 72 hours, while IL-4, at 48 hours.

EAE induction and treatment protocols

Female C57BL/6J mice, 6 to 8 weeks old, were purchased from Harlan Italy (S. Pietro al Natisone, Italy). All animals were housed in pathogen-free conditions and treated according to the guidelines of the Animal Ethical Committee of our Institute. Mice were immunized according to a previously published protocol[20] with incomplete Freund adjuvant (IFA; Difco, Detroit, MI) containing 4 mg/mL *Mycobacterium tuberculosis* (strain H37Ra; Difco) and 200 μg MOG35-55 (Espikem). Immunization with MOG35-55 was followed by intravenous administration of 400 ng pertussis toxoid (Sigma-Aldrich) on day 0 and after 48 hours. To test the efficacy of MSCs, we used 2 different administration protocols. In the preventive protocol, mice received intravenous 1 × 10^6 MSCs diluted in PBS without Ca^{2+} and Mg^{2+} (Sigma-Aldrich) on days 3 and 8 after immunization. Controls received intravenous injections of an equal volume of PBS at the same time points. In the therapeutic protocol, mice were injected with the same amount of cells on day 10, 15, or 24 after immunization. Weight and clinical score were recorded daily. Clinical score was assigned according to a standard and validated 0 to 5 scale.[20] Mice were followed, unless moribund, for at least 40 days following immunization. Disease incidence, onset, and maximum score were recorded for each mouse and expressed as mean ± SD. The cumulative disease score was calculated by summing the neurologic scores recorded daily for each mouse along the whole period of observation.

Histology

At time of death, mice were transcardially perfused with 4% paraformaldehyde. Brains and spinal cords were removed and postfixed in the same fixative for 2 to 4 hours, washed in PBS, and then embedded in paraffin. Sections were cut at 5 μm on a microtome and stained for histologic examination under an Olympus Provis AX70 (Olympus, Italia Segrate, MI) optical microscope. Objectives used were

Olympus UPlanFl 4 ×/0.13 NA, 10 ×/0.30 NA, 20 ×/.50 NA, and 40 ×/0.75 NA. Hematoxylin and eosin (HE) staining was used to reveal perivascular inflammatory infiltrates, and Luxol Fast Blue (LFB) staining, for demyelination. T cells were stained using a rat anti-CD3 antibody (pan–T-cell marker; Serotec), and macrophages, with a peroxidase-labeled rat anti–Mac-3 antibody (Pharmingen Becton Dickinson), both revealed with a biotin-labeled secondary antirat antibody (Serotec). All primary antibodies were revealed using biotin-labeled or rhodamine-labeled secondary antibodies. CNS pathologic score was calculated on an average of 6 CNS tissue sections per mouse (at 100 × magnification) and expressed as mean ± SD. In each section, we determined the total number of positive elements and reported it as number of positive elements/mm^2. Spinal cord demyelination was scored as it follows: 1 = traces of subpial demyelination; 2 = marked subpial and perivascular demyelination; 3 = confluent perivascular or subpial demyelination; 4 = massive perivascular and subpial demyelination involving one half of the spinal cord with presence of cellular infiltrates in the CNS parenchyma; and 5 = extensive perivascular and subpial demyelination involving the whole cord section with presence of cellular infiltrates in the CNS parenchyma. Data were stored on a computer using an Olympus DP70 digital camera using the acquisition software Image-Pro Plus (Media Cybernetics, Silver Spring, MD).

Immunofluorescence

eGFP-positive cells were tracked exclusively inside the secondary lymphoid organs and the CNS one day after MSC injection, before disease onset (day 9 after immunization), or 40 days after immunization when disease reached a chronic phase. At the time of death, mice injected with eGFP$^+$ MSCs were transcardially perfused with 4% paraformaldehyde. Brain, spleen, lymph nodes, and spinal cord were removed, washed in PBS, and then embedded in Tissue-Tek optimal cutting temperature (OCT) compound (Sakura Finetek Europe, Zoeter Woude, The Netherlands). Sections were cut at 6 μm on a cryostat and stained for immunofluorescence examination. Slides were brought to RT, fixed in acetone at 4°C for 10 minutes, and then placed in PBS for 5 minutes to remove Tissue-Tek OCT. All slides were blocked with 5% BSA in PBS for 30 minutes. Endogenous peroxidase was blocked with the methanol and hydrogen peroxidase for 20 minutes. Slides were washed 3 times for 5 minutes each in PBS before being probed with a rabbit anti-GFP antibody (Molecular Probes, Eugene, OR) overnight in a humidified chamber at 4°C. After incubation for 30 minutes with an antirabbit secondary antibody conjugated with Alexa 488 (Molecular Probes), slides were washed 3 times for 5 minutes in PBS. To detect the cell nucleus, cells were stained with 4′,6-diamidino-2-phenylindole (DAPI; Sigma-Aldrich) for 5 minutes and then mounted with glycerol buffered with PBS. To detect T cells and macrophages, slides were stained as described before and revealed with an antirat antibody conjugated with Alexa 594 (Molecular Probes).

Results

Isolation of stable MSCs

MSCs, devoid of hematopoietic markers, were obtained from the bone marrow of C57BL/6J healthy mice after 4 to 5 cycles of culture and expressed a stable CD45$^-$CD34$^-$CD11b$^-$CD9$^+$Sca-1$^+$CD44$^+$ phenotype. Variable levels of CD73$^+$ (38%-73%) and MHC class I (29%-61%) were detected. In contrast, no MHC class II, CD80, CD86, CD40, and leukocyte function antigen 3 (LFA3) were detected in resting conditions (data not shown). This phenotype was maintained in culture for up to 40 passages (more than 6 months).

MSCs suppress T-cell activation

In order to confirm that MSCs are able to suppress T-cell activation, we challenged T cells from healthy C57BL/6J mice with different antigenic stimuli in the presence or absence of MSCs. MSCs inhibited T cells activated with anti-CD3 alone or in combination with anti-CD28 (Figure 1A). Likewise, MSCs inhibited the specific response to the encephalitogenic MOG35-55 peptide by T cells obtained from MOG-immunized mice (Figure 1B). Similar results were obtained when a non–T-cell receptor (TCR)–mediated mitogenic stimulus such as ConA was used (Figure 1C). Since maximal inhibition of T-cell proliferation was already obtained at an MSC concentration of 0.25 × 10^5, this concentration was used for all the following experiments in vitro unless specified (Figure 1C). As the effect of MSCs has been claimed to be dependent on cell-to-cell interaction but also on the production of soluble factors,[10,13,14] we stimulated T cells with anti-CD3 or ConA in the presence or absence of supernatants from MSC culture at confluence. MSC supernatants significantly inhibited TCR-dependent and -independent proliferation almost to levels observed when MSCs were added to the well of proliferating T cells (Figure 1D). Previous reports demonstrated that MSCs are ignored by alloreactive T cells probably due to their lack of surface costimulatory molecules.[9,12,21,22] Thus, we added MSCs to murine or human MLR to verify whether our cells could also inhibit T-cell activation in an allo- or xeno-reactive setting. Indeed, MSCs inhibited proliferation of syngenic effector T cells from C57BL/6J to irradiated MNCs from a CD1 mouse (Figure 2A). Such effect was observed also when we used allogenic CD1 T cells as effector cells in response to irradiated C57BL/6J feeders (Figure 2B). Of relevance, a marked inhibitory effect was observed when MSCs were added to a human MLR supporting a suppressive activity acting beyond species barriers (Figure 2C). MSC inhibition of T-cell proliferation was paired by a dose-dependent decrease of IFN-gamma and TNF-alpha production (Figure 2D). IL-4 production by activated T cells cocultured with MSCs was unaffected (not shown).

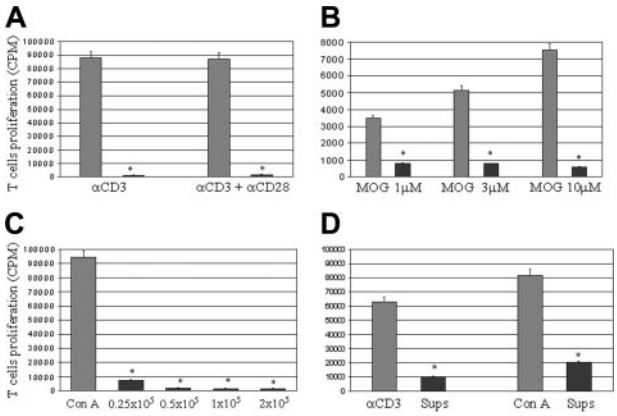

Figure 1. MSCs inhibit T-cell activation. (A) Murine MSCs (mMSCs) inhibit T-cell proliferation upon stimulation with anti-CD3 with or without costimulatory trigger, (B) with the encephalitogenic MOG35-55 peptide, and (C) with ConA. (D) A remarkable inhibition is obtained also with the supernatant from MSC cultures at confluence. ▨ indicates T cells stimulated in the absence of MSCs; ■, T cells treated with 0.25 × 10^5 MSCs (A-B), increasing doses of MSCs (C), or MSC-derived supernatant (D). *$P < .05$ by Mann-Whitney U test. Error bars indicate SD values. Proliferative responses are expressed as mean counts per minute (CPM) of at least 3 independent experiments. Sups indicates supernatants.

T-cell reactivity is retrieved by administration of IL-2

Next, we sought to verify whether inhibition of T-cell proliferation by MSCs was due to cell death resulting from the induction of apoptosis. MSCs did not significantly increase the percentage of annexin V–positive T cells upon stimulation with anti-CD3 or ConA ($P < .2$, Figure 2E). These results confirm that most of the MSC-treated T cells are unresponsive and unable to proliferate but still viable. Nevertheless, inhibition of T-cell proliferation by MSCs was partially reversed by the administration of IL-2;

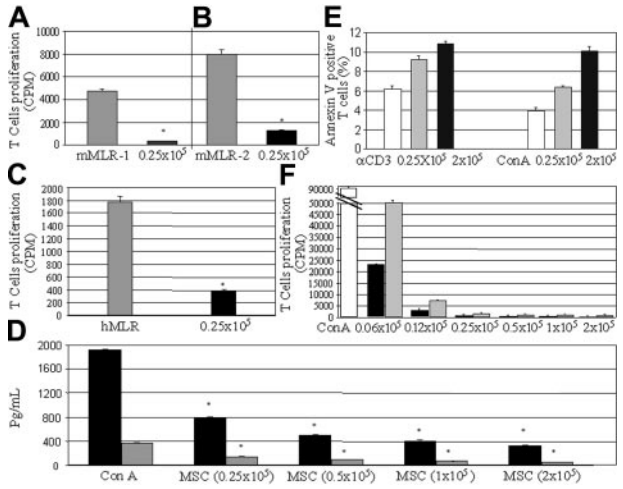

Figure 2. MSCs are viable but anergic. MSCs from C57BL/6J mice inhibit proliferation of effector T cells from C57BL/6J mice in response to irradiated MNCs from CD1 mice (A), of effector cells from CD1 mice to irradiated C57BL/6J feeders (B), and of effector human PBMCs to allogeneic irradiated human feeder cells (C). (A-C) ▨ indicates T cells stimulated in the absence of MSCs; ■, MSC-treated T cells. *$P < .05$ by Mann-Whitney *U* test. Error bars indicate SD values. Proliferative responses are expressed as mean CPM of at least 3 independent experiments. hMLR indicates human MLR. (D) MSCs inhibit production of IFN-gamma (■) and TNF-alpha (▨) by ConA-stimulated T cells in a dose-dependent manner. *$P < .05$ by Mann-Whitney *U* test compared with cytokine levels induced by ConA stimulation. Columns represent the mean ± SD from at least 3 separate experiments. MSCs do not significantly increase ($P < .2$ by Mann-Whitney *U* test) the percentage of apoptotic T cells upon anti-CD3 or ConA stimulation (E). (E) □ indicates T cells stimulated in the absence of MSCs; ▨, with 0.25×10^5 MSC-treated T cells; and ■,with 2×10^5 MSC-treated T cells. Bars represent the mean ± SD percent variation (n = 3) of annexin V–positive cells. The inhibition of proliferation induced by ConA stimulation is partially reverted by the administration of 100 IU/mL IL-2. Such an effect is more pronounced at lower MSC concentrations but still enough to increase by about 2-fold CPM at each concentration (F). (F) □ indicates conA-stimulated T cells; ■, MSC-treated T cells; and ▨, IL-2–stimulated MSC-treated T cells. Results are expressed as mean CPM ± SD of at least 3 independent experiments.

this effect was more evident at lower MSC concentration (Figure 2F). These findings suggest that upon MSC coculture, T cells are alive but in moderate state of anergy that can be partially reverted by IL-2.

Administration of MSCs ameliorates EAE

Due to the striking inhibition of T-cell activation, we sought to address whether MSCs could affect a prototypical T-cell–mediated autoimmune disease such as EAE. In a preventive protocol, MSCs intravenously injected at day 3 and day 8 after immunization strikingly reduced disease severity, reaching statistical significance from day 17 onward compared with control mice ($P < .05$ by Mann-Whitney *U* test) (Figure 3A). We did not observe any effect on disease onset. Injection of unpurified marrow cells at the same time points resulted in scores comparable with control mice (not shown). The clinical effect of MSCs was associated with a straightforward reduction of demyelination both in the brain and spinal cord of treated mice (Table 1; Figure 4). In the MSC-treated animals, we detected a remarkable decrease of T cells and macrophages infiltrating the CNS parenchyma compared with controls (Table 1; Figure 4). In the same experiment, we sought to evaluate whether the administration of MSCs after disease onset was still as effective as EAE treatment. Therefore, we administered MSCs at day 24, upon disease stabilization, a time point that resulted as an appropriate time window for the intravenous administration of neural stem cells in EAE.[20] MSCs administered at day 24 did not have any clinical effect (Figure 3A), as disease and pathology scores were similar to those of controls (Table 1). To evaluate the effect of the administration of MSCs at an earlier time point after disease onset, we injected MSCs either at disease onset (at the occurrence of the first symptoms of disease, around day 10) or at the peak of disease (day 15). Both treatments halted disease progression when compared with vehicle alone–treated controls (Figure 3B), resulting in a statistically significant reduction of cumulative disease score (Table 1). Similar to that observed in mice treated before disease onset, we observed a significant reduction of demyelination and infiltrates of macrophages and T cells in the CNS compared with controls (Table 1; Figure 5). MSC-treated mice did not show any increased frequency of concomitant infectious diseases or cancer along a maximum observation period of 3 months. Hence, MSCs are effective in treating EAE both before and after disease onset but do not seem to induce a state of immunodeficiency.

MSC administration induces T-cell anergy in vivo

To verify whether MSCs affect the capacity of T cells from treated animals to mount an appropriate response upon stimulation, we dissected T-cell responses to mitogens and MOG35-55 from treated animals and EAE-affected control mice. In the MSC-treated mice, the proliferative response to MOG35-55, anti-CD3/anti-CD28, and ConA was inhibited compared with control mice (Figure 6A). The suppression of this response was abrogated upon in vitro administration of IL-2, supporting a tolerogenic activity of MSCs leading to T-cell anergy (Figure 6B). To verify whether the induction of anergy was exclusively dependent on the inhibition of T-cell activation or on the simultaneous induction of cells with a suppressive activity, we checked for the presence of $CD4^+CD69^-CD25^+$ regulatory T cells (TREGs) in the lymphoid organs of affected mice. Given that the analysis was performed after immunization with MOG, most effector cells are known to be $CD4^+CD25^+CD69^+$. Thus, gating exclusively on $CD4^+CD69^-$ cells, we were confident to detect true T-^{regs}. We did not observe any difference in the percentage of $CD4^+CD69^-CD25^+$ T-^{regs} among T cells recovered from the spleen of MSC-treated mice and controls ($P < .2$, Figure 6C). In addition, we also verified whether the in

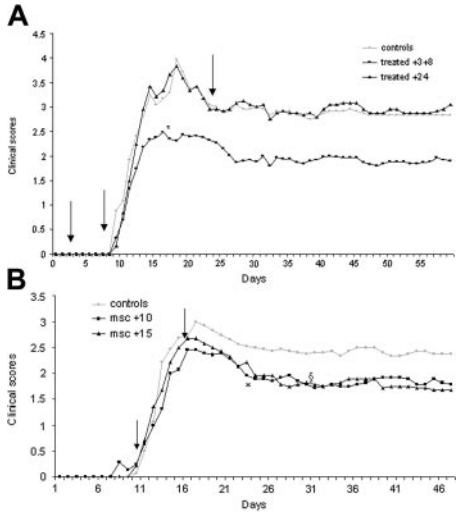

Figure 3. Intravenous injection of MSCs ameliorates EAE. MSCs injected at days 3 and 8 after immunization (■) halt disease severity compared with controls (△) ($P < .05$ from day 17 onward). No differences were observed between controls and mice treated at day 24 after immunization (▲) (A). Administration of MSCs at day 10 (■) or at day 15 (▲) after immunization, after disease onset, ameliorates EAE ($P < .05$ from day 22 [*] for mice treated at day 10 and from day 30 [§] for mice treated at day 15 compared with controls [△] by Mann-Whitney *U* test) (B). Arrows indicate days of MSC injection.

Table 1. Clinical-pathologic features of EAE-affected mice

	Disease incidence, no./no. total (%)	Disease onset, d after immunization (range)	Mean maximum neurologic score (range)	Cumulative disease score	Demyelination score (range)	Macrophages, cells/mm^2 (range)	CD3$^+$, cells/mm^2 (range)
Controls	6/6 (100)	9.8 ± 1.0 (9-11)	3.9 ± 0.9 (2-5)	149.0 ± 46.8	3.8 ± 1.3 (2-6)	94.8 ± 34.5 (40-190)	146.2 ± 35.7 (71-200)
Treated, d +3 and d +8	15/15 (100)	10.1 ± 1.2 (9-13)	3.1 ± 1.1 (1-5)	101.2 ± 48.6†	1.9 ± 1.2† (1-5)	52.7 ± 27.2† (20-134)	54.7 ± 21.3† (22-103)
Treated, d +24	6/6 (100)	10.0 ± 0.9 (9-11)	4.0 ± 0.6 (3-5)	150.7 ± 49.7	3.2 ± 1.4 (1-6)	89.9 ± 26.9 (42-132)	107.7 ± 25.4 (73-155)
Controls	8/8 (100)	10.4 ± 0.6 (9-12)	3.2 ± 0.4 (2.5-4)	122.8 ± 17.8	6.1 ± 1.86 (2-8)	110.0 ± 21.9 (65-138)	123.8 ± 22.0 (71-158)
Treated, d +10	7/8 (88)	9.7 ± 1.8 (7-14)	2.8 ± 0.3 (2-3.5)	98.1 ± 14.3*	2.5 ± 1.3† (1-5)	52.7 ± 15.0† (34-87)	74.7 ± 17.4† (51-112)
Treated, d +15	7/8 (88)	10.3 ± 0.9 (9-12)	2.8 ± 0.3 (2-3.5)	94.2 ± 15.3	3 ± 2.2* (1-8)	66.9 ± 12.7† (48-88)	84.9 ± 19.9† (58-117)

Two entries for controls reflect two sets of experiments as described in "Materials and methods" (preventive and therapeutic protocols) and "Results" (see Figures 3-5).
*$P < .05$ (Mann-Whitney test).
†$P < .01$ (Mann-Whitney test).

vivo administration of MSCs could affect antigen-presenting cells in lymphoid organs. Therefore, we analyzed the expression of classes I and II, CD80, and CD40 molecules on CD11c DCs from the spleen of affected mice. We observed that in MSC-treated mice, only CD40 and class II molecules are modestly down-regulated compared with control mice ($P < .2$, Figure 6D). Thus, the in vivo effect of MSCs is likely to be due to the induction of IL-2–reversible T-cell anergy, and we cannot support an MSC-induced impairment of antigen presentation within the lymphoid organs.

eGFP-engineered MSCs are detected in the lymphoid organs and in the spinal cord of EAE-affected mice

Based on the results of the in vivo experiments suggesting a clear clinical advantage with MSCs administered early after disease onset, we postulated that MSCs actively interfere with the generation of effector T cells. To prove this hypothesis, we administered eGFP-positive MSCs at day 3 and day 8 after immunization and carefully tracked them in the lymphoid organs and the CNS. First, we demonstrated that transfection with eGFP did not affect the MSC phenotype and their in vitro immunosuppressive activity (data not shown). eGFP$^+$ MSCs were detected at day 9 after immunization in the spleen and draining lymph nodes (Figure 7A-B), often in close relationship with T cells (Figure 7D). At this time, we could not observe eGFP$^+$ cells in the CNS. In contrast, a large number of eGFP$^+$ MSCs were detected at day 40 in the subarachnoid space of the spinal cord of MSC-treated mice (Figure 7G-H). Very rare eGFP$^+$ cells were observed inside the parenchyma just beneath the subpial layer. At this time, still large numbers of eGFP$^+$ MSCs were observed infiltrating the spleen (Figure 7E). These findings suggest that upon intravenous administration, MSCs rapidly migrate to lymphoid organs where they are likely to interact with activated T cells and exert their immunoregulatory activity.

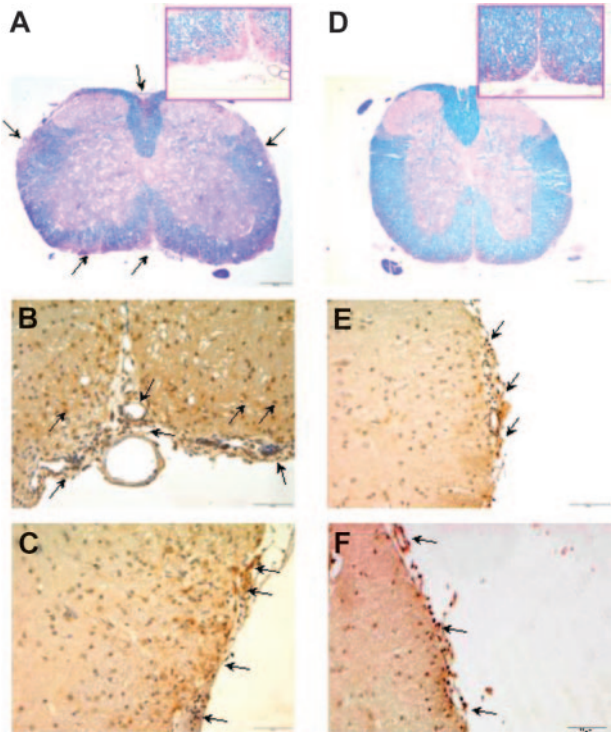

Figure 4. Pathologic findings in the CNS of C57BL/6J mice immunized with MOG35-55. Control mice are shown in panels A-C, while animals treated at 3 and 8 days after immunization are shown in panels D-F. LFB staining of the spinal cord shows areas of demyelination (arrows) in control mice compared with MSC-treated mice (D) (4 ×). CD3$^+$ T cells (B) and macrophages (C) infiltrating the spinal cord close to leptomeningeal vessels of control mice are shown (10 ×). Limited CD3$^+$ T cells (E) and macrophages (F) are observed in the spinal cord from MSC-treated mice. Control mice were immunized with MOG35-55 and treated with intravenous PBS alone. Arrows indicate representative histological abnormalities.

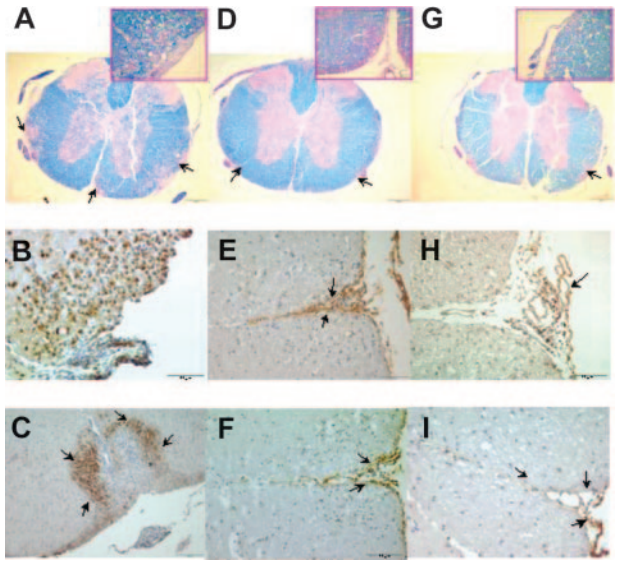

Figure 5. Pathologic findings in the CNS of C57BL/6J mice immunized with MOG35-55. Control mice are shown in panels A-C, while animals treated at 10 days after immunization are shown in panels D-F and at 15 days after immunization are shown in panels G-I. LFB staining of spinal cord shows large areas of demyelination in the control mice (A) but only scattered foci in the MSC-treated mice (D,G) (4 ×). CD3$^+$ T cells (B, 20 ×) and macrophages (C) infiltrate the subpial layer of the spinal cord of control mice (10 ×). In contrast, only few T cells (E,H) and macrophages (F,I) are detected in the spinal cord from MSC-treated mice (all 10 ×). Control mice were immunized with MOG35-55 and treated with intravenous PBS alone. Arrows indicate representative histological abnormalities.

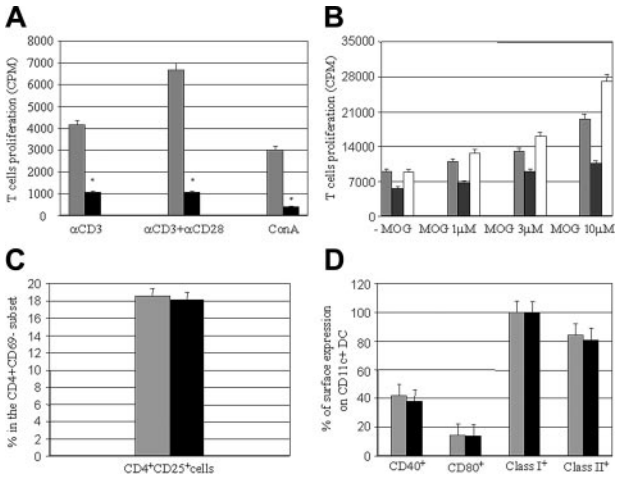

Figure 6. In vivo, MSCs induce T-cell anergy but do not affect TREGs and DCs. T cells from the spleen and lymph nodes of mMSC-treated mice are unresponsive upon anti-CD3, anti-CD3/anti-CD28, and ConA (■) compared with control mice (▨) (A, $*P < .05$ Mann-Whitney *U* test). Following in vitro administration of IL-2, T cells from mMSC-treated mice proliferated upon MOG stimulation to levels comparable with T cells from control mice. ▨ indicates MOG-stimulated T cells; ■, mMSC-treated T cells; and □, IL-2–stimulated mMSC-treated T cells (B). Proliferative responses are expressed as mean CPM ± SD of at least 3 independent experiments. (C) The proportion of $CD4^+CD25^+$ TREGs within $CD4^+CD69^-$ population of the spleen of control (▨) and MSC-treated (■) mice. $P < .2$ by Mann-Whitney *U* test. Bars represent the mean ± SD percent variation (n = 4) of TREGs. (D) The frequency of costimulatory and class I and class II molecules on $CD11c^+$ DCs from the spleen of control mice (▨) and MSC-treated mice (■). $P < .2$ by Mann-Whitney *U* test. Columns represent the mean ± SD percent variation of at least 3 separate experiments. Control mice were immunized with MOG35-55 and treated with intravenous PBS alone.

Discussion

In this report, we demonstrated that autologous murine MSCs can be used to treat EAE, a T-cell–mediated model for CNS-directed autoimmunity, and that such beneficial effect is achieved by means of a potent suppression of T-cell response. MSCs have been recently reported to have an anti-inflammatory potential in experimental models of acute pulmonary[23] and renal injury.[24] Indeed, human MSCs have been shown to exert a profound inhibition on activated T cells when stimulated by allogenic or mitogenic stimuli.[10,12,21] This effect has been achieved both coculturing MSCs with activated T cells and when MSC/T-cell direct interaction was prevented, thus suggesting that for T-cell suppression both cell-to-cell contact and soluble factors are required. Among the latter, tumor growth factor β1 (TGF β1), hepatocyte growth factor (HGF),[10] prostaglandin E2,[13] and indoleamine 2,3-dioxygenase[14] are consistent candidates. The immunologic properties of murine MSCs have been evaluated by Krampera et al who showed that MSCs also suppress the response to cognate antigens.[25] More recently, the same group has shown that murine T cells stimulated in the presence of MSCs are only transiently arrested during their division cycle.[26] In our study, we have shown that MSCs can suppress T-cell proliferative response against TCR-dependent and -independent polyclonal stimuli. Such effect was obtained by adding MSCs to T cells in culture but also through the administration of the supernatant of MSCs. These findings suggest that both soluble factors and cell-contact mechanisms affect T-cell functions and that the suppressive effect is not dependent on T-cell starvation by competitor cells such as MSCs. Such effect was paralleled by a significant suppression of IFN-gamma and TNF-alpha production by activated T cells, supporting a profound inhibition of the T helper 1 (Th1) response by MSCs. In addition, the inhibitory effect on T-cell response in vitro was partially restored by the administration of IL-2. We could not detect any increase of apoptotic T cells when they were stimulated with ConA or anti-CD3 in the presence of MSCs, thus confirming that MSCs do not induce T-cell apoptosis.[10] Together with such immune-suppressive activity, it has been reported that MSCs do not elicit proliferative responses when cocultured with allogenic T cells,[9,12] even upon differentiation.[22] It is likely that such effect may be related to the limited surface expression of MHC class II molecules on resting condition but mostly on the complete lack of costimulatory molecules such as CD80, CD86, and CD40.[12,22] In this study, we confirmed that MSCs fail to express class II and costimulatory molecules and also that MSCs are "ignored" by allogenic T cells when used to suppress proliferation of T cells in murine MLR. The escape from T-cell–mediated responses is further confirmed by the surprising capacity of MSCs to inhibit human MLR without generating a xeno-response, thus supporting a possible role for such cells as therapy in an allogenic environment.

Based on these findings, we administered MSCs with the aim of curing EAE, a prototypical T-cell–mediated autoimmune disease of the CNS. Administration of MSCs before EAE onset successfully ameliorated severity of disease. Similarly, MSCs were also effective if administered early during disease course or at peak of disease. Clinical efficacy for both treatments was demonstrated by a decreased mean maximum score and cumulative disease score that were consistent with a milder neurologic impairment. Such results were sustained by reduced demyelination and cellular infiltrates. Conversely, we could not detect any improvement of clinical or histologic scores when MSCs were injected after disease reached a chronic phase. These results are consistent with an effect occurring during the early inflammatory phase of disease, supporting the possibility that MSCs could affect the generation of encephalitogenic effector T cells. Thus, we addressed whether intravenously injected MSCs can modulate T-cell responses within the peripheral compartment of EAE-affected mice. Indeed, we observed a striking inhibition of T-cell proliferation from MSC-treated mice, upon stimulation with the encephalitogenic MOG

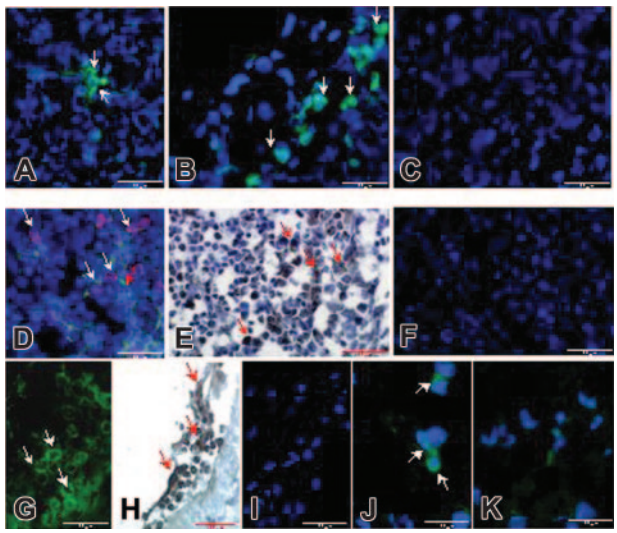

Figure 7. MSCs home to lymphoid organs and the subarachnoid spaces. $eGFP^+$ mMSCs are detected, at day 9 after immunization, in the spleen of treated mice by immunofluorescence as shown in panels A-B (20 ×) and, at day 40 after immunization, as detected by immunohistochemistry (brown, E) (20 ×). $eGFP^+$ mMSCs are observed next to T cells as revealed by triple staining for CD3 (red), DAPI (blue), and $eGFP^+$ (green) in the spleen of treated animals (D) (20 ×). $eGFP^+$ mMSCs are detected also in the subarachnoid spaces of the spinal cord of MSC-treated mice by immunofluorescence (G) and immunohistochemistry (H). Scattered $eGFP^+$ cells are observed by immunofluorescence inside the parenchyma just beneath the subpial layer of treated mice (J) (40 ×). Negative controls are shown in panels C, F, I, and K. Arrows indicate MSCs.

peptide but also with polyclonal mitogenic stimuli. This effect was fully reverted by the administration of IL-2. Such result is partially in contrast with the results by Glennie et al who reported that IL-2 could restore IFN-gamma production but not proliferation of T cells anergized by MSCs in vitro.[26] Nevertheless, we believe that data from Glennie et al's work are indeed in line with the partial recovery of T-cell proliferation that we observed upon IL-2 administration in vitro, which was clearly dependent on MSC/T-cell ratio (Figure 4B). Thus, such a result is likely to be related to a milder tolerogenic effect of MSCs when administered in vivo compared with a more potent suppression obtained in vitro where a much higher MSC/T-cell ratio is achieved. As peripheral tolerance could be maintained by TREGs,[27] we sought to verify whether MSCs could induce T-^{regs} upon in vivo administration. Similar levels of $CD4^+CD69^-CD25^+$ T-^{regs} were detected in the secondary lymphoid organs from control mice and MSC-treated mice, thus confirming that MSC inhibitory effect is not dependent on TREGs.[25] Next, we analyzed the effect of the in vivo administration of MSCs on DCs from the spleen of treated mice, and we detected only a limited down-regulation of MHC class II molecules and CD40, suggesting the possibility that an impaired costimulation by DCs from MSC-treated mice could also contribute to the generation of peripheral T-cell anergy.[28] As it has been recently suggested that MSCs may alter DC maturation and impair their function,[29,30] more studies will have to address the in vivo effect of MSCs on the induction of peripheral tolerance by DCs.

Last, we sought to demonstrate that this suppression is truly occurring at the level of the lymphoid organs where T-cell priming occurs. Upon MSC transfection with eGFP, we detected high numbers of eGFP-tagged MSCs within the spleen and draining lymph nodes from treated mice before and after disease onset. $eGFP^+$ cells were often next to T cells. A substantial number of $eGFP^+$ MSCs were also observed in the subarachnoid space of the spinal cord but only rarely inside the parenchyma of MSC-treated mice and only in mice killed after 40 days. These findings may suggest that MSCs may interact with immune cells also at one of the sites where T cells enter the CNS.[31,32] These results could be explained by the fact that the substantial efficacy of MSCs as treatment for EAE resulted in a limited damage inside the CNS parenchyma, thus preventing the migration of MSCs to provide repair. More likely, it may be necessary to wait to achieve full engraftment of MSCs inside the CNS.

Overall, the results described in this study support for the first time the use of MSCs in the treatment of autoimmunity due to a profound suppression on effector T cells and the induction of peripheral tolerance. As human MSCs have already been used for the treatment of acute graft-versus-host disease,[16-18] these findings open a new perspective for the treatment of multiple sclerosis.

References

1. Caplan AI. Mesenchymal stem cells. J Orthop Res. 1991;9:641-650.
2. Pittenger MF, Mackay AM, Beck SC, et al. Multilineage potential of adult human mesenchymal stem cells. Science. 1999;284:143-147.
3. Eglitis MA, Mezey E. Hematopoietic cells differentiate into both microglia and macroglia in the brains of adult mice. Proc Natl Acad Sci U S A. 1997;94:4080-4085.
4. Kopen GC, Prockop DJ, Phinney DG. Marrow stromal cells migrate throughout forebrain and cerebellum, and they differentiate into astrocytes after injection into neonatal mouse brains. Proc Natl Acad Sci U S A. 1999;96:10711-10716.
5. Jiang Y, Jahagirdar BN, Reinhardt RL, et al. Pluripotency of mesenchymal stem cells derived from adult marrow. Nature. 2002;418:41-49.
6. Mezey E, Chandross KJ, Harta G, Maki RA, McKercher SR. Turning blood into brain: cells bearing neuronal antigens generated in vivo from bone marrow. Science. 2000;290:1779-1782.
7. Brazelton TR, Rossi FMV, Keshet GI, Blau HM. From marrow to brain: expression of neuronal phenotypes in adult mice. Science. 2000;290: 1775-1779.
8. Li Y, Chen J, Chen XG, et al. Human marrow stromal cell therapy for stroke in rat: neurotrophins and functional recovery. Neurology. 2002;59:514-523.
9. Bartholomew A, Sturgeon C, Siatskas M, et al. Mesenchymal stem cells suppress lymphocyte proliferation in vitro and prolong skin graft survival in vivo. Exp Hematol. 2002;30:42-48.
10. Di Nicola M, Carlo-Stella C, Magni M, et al. Human bone marrow stromal cells suppress T-lymphocyte proliferation induced by cellular or nonspecific mitogenic stimuli. Blood. 2002;99: 3838-3843.
11. Krampera M, Glennie S, Dyson J, et al. Bone marrow mesenchymal stem cells inhibit the response of naive and memory antigen-specific T cells to their cognate peptide. Blood. 2002;101: 3722-3729.
12. Tse WT, Pendleton JD, Beyer WM, Egalka MC, Guinan EC. Suppression of allogeneic T-cell proliferation by human marrow stromal cells: implications in transplantation. Transplantation. 2003;75:389-397.
13. Aggarwal S, Pittenger MF. Human mesenchymal stem cells modulate allogeneic immune cell responses. Blood. 2004;105:1815-1822.
14. Meisel R, Zibert A, Laryea M, Gobel U, Daubener W, Dilloo D. Human bone marrow stromal cells inhibit allogeneic T-cell responses by indoleamine 2,3-dioxygenase mediated tryptophan degradation. Blood. 2004;103:4619-4621.
15. Lazarus HM, Haynesworth SE, Gerson SL, Rosenthal NS, Caplan AI. Ex vivo expansion and subsequent infusion of human bone marrow-derived stromal progenitor cells (mesenchymal progenitor cells): implications for therapeutic use. Bone Marrow Transplant. 1995;16:557-564.
16. Frassoni F, Labopin M, Bacigalupo A, et al. Expanded mesenchymal stem cells (MSC), co-infused with HLA identical hematopoietic stem cell transplants, reduce acute and chronic graft-versus-host disease: a matched pair analysis [abstract]. Bone Marrow Transplant. 2002;29(suppl 2). Abstract 52.
17. Le Blanc K, Rasmusson I, Sundberg B, et al. Treatment of severe acute graft-versus-host disease with third party haploidentical mesenchymal stem cells. Lancet. 2004;363:1439-1441.
18. Bacigalupo A, Palandri F. Management of acute graft versus host disease (GvHD). Hematol J. 2004;5:189-196.
19. Follenzi A, Ailles LE, Bakovic S, Geuna M, Naldini L. Gene transfer by lentiviral vectors is limited by nuclear translocation and rescued by HIV-1 pol sequences. Nat Genet. 2000;25:217-222.
20. Pluchino S, Quattrini A, Brambilla E, et al. Injection of adult neurospheres induces recovery in a chronic model of multiple sclerosis. Nature. 2003; 422:688-694.
21. Le Blanc K, Tammik L, Sundberg B, Haynesworth SE, Ringden O. Mesenchymal stem cells inhibit and stimulate mixed lymphocyte cultures and mitogenic responses independently of the major histocompatibility complex. Scand J Immunol. 2003;57:11-20.
22. Le Blanc K, Tammik C, Rosendahl K, Zetterberg E, Ringden O. HLA expression and immunologic properties of differentiated and undifferentiated mesenchymal stem cells. Exp Hematol. 2003;31: 890-896.
23. Ortiz LA, Gambelli F, McBride C, et al. Mesenchymal stem cell engraftment in lung is enhanced in response to bleomycin exposure and ameliorates its fibrotic effects. Proc Natl Acad Sci U S A. 2003;100:8407-8411.
24. Togel F, Hu Z, Weiss K, Isaac J, Lange C, Westenfelder C. Administered mesenchymal stem cells protect against ischemic acute renal failure through differentiation-independent mechanisms. Am J Physiol Renal Physiol. 2005 Feb 15;Epub ahead of print.
25. Krampera M, Glennie S, Dyson J, et al. Bone marrow mesenchymal stem cells inhibit the response of naive and memory antigen-specific T cells to their cognate peptide. Blood. 2003;101: 3722-3729.
26. Glennie S, Soeiro I, Dyson PJ, Lam EW, Dazzi F. Bone marrow mesenchymal stem cells induce division arrest anergy of activated T cells. Blood. 2005;105:2821-2827.
27. O'Garra A, Vieira P. Regulatory T cells and mechanisms of immune system control. Nat Med. 2004;10:801-805.
28. Schwartz RH. T cell anergy. Ann Rev Immunol. 2003;21:305-334.
29. Beyth S, Borovsky Z, Mevorach D, et al. Human mesenchymal stem cells alter antigen-presenting cell maturation and induce T cell unresponsiveness. Blood. 2005;5:2214-2219.
30. Jiang XX, Zhang Y, Liu B, et al. Human mesenchymal stem cells inhibit differentiation and function of monocyte-derived dendritic cells. Blood. 2005;105:4120-4126
31. Ransohoff RM, Kivisakk P, Kidd G. Three or more routes for leukocyte migration into the central nervous system. Nat Rev Immunol. 2003;3:569-581.
32. Magliozzi R, Columba-Cabezas S, Serafini B, Aloisi F. Intracerebral expression of CXCL13 and BAFF is accompanied by formation of lymphoid follicle-like structures in the meninges of mice with relapsing experimental autoimmune encephalomyelitis. J Neuroimmunol. 2004;148:11-23.